THE JOURNAL OF PHYSICAL CHEMISTRY Letters

Perspective

pubs.acs.org/JPCL

Material Innovation in Advancing Organometal Halide Perovskite Functionality

Fan Zheng,[†] Diomedes Saldana-Greco,[†] Shi Liu,[†,‡] and Andrew M. Rappe*[,†]

[†]The Makineni Theoretical Laboratories, Department of Chemistry, University of Pennsylvania, Philadelphia, Pennsylvania 19104−6323, United States

[‡]Geophysical Laboratory, Carnegie Institution for Science, Washington, DC 20015, United States

ABSTRACT: Organometal halide perovskites (OMHPs) have garnered much attention recently for their unprecedented rate of increasing power conversion efficiency (PCE), positioning them as a promising basis for the next-generation photovoltaic devices. However, the gap between the rapid increasing PCE and the incomplete understanding of the structure−property−performance relationship prevents the realization of the true potential of OMHPs. This Perspective aims to provide a concise overview of the current status of OMHP research, highlighting the unique properties of OMHPs that are critical for solar applications but still not adequately explained. Stability and performance challenges of OMHP solar cells are discussed, calling upon combined experimental and theoretical efforts to address these challenges for pioneering commercialization of OMHP solar cells. Various material innovation strategies for improving the performance and stability of OMHPs are surveyed, showing that the OMHP architecture can serve as a promising and robust platform for the design and optimization of materials with desired functionalities.

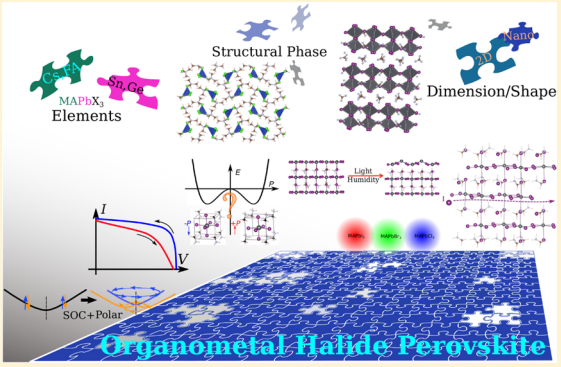

Organometal halide perovskites (OMHPs), with their unprecedented rate of increasing power conversion efficiency (PCE) over the past five years,[1] have transformed photovoltaic (PV) research and development. These materials, especially methylammonium lead iodide ($MAPbI_3$), have shown appropriate band gaps in the visible light region,[2,3] strong light absorption,[4,5] long carrier lifetime, and high carrier mobility,[6−8] making them ideal for PV materials. The permanent dipole afforded by the organic molecule (MA) is suggested to give rise to ferroelectricity, and the strong spin−orbit coupling (SOC) carried by the heavy atoms (Pb and I) introduces additional spin-related effects. The OMHP architecture therefore provides a tremendous capacity to tune the structural, electronic, optical, and magnetic properties to achieve various important functionalities.[9]

However, many challenges remain. The most fundamental one is the gap between the rapidly increasing PCE and the incomplete understanding of the structure−property−performance relationship, which hinders the realization of the true potential of OMHPs. Specifically, the determination of the PCE for OMHP-based solar cell is ambiguous due to the strong current−voltage (I−V) hysteresis, whose origin (intrinsic and extrinsic) is not clear. The relatively weak stability of $MAPbI_3$ (decomposes rapidly with exposure to water and light) strongly reduces the robustness of OMHP solar cells. Moreover, fundamental questions such as the ferroelectricity and the role of SOC in carrier dynamics are still elusive. Therefore, innovative routes of manipulating these materials are motivated not only to enhance performance and durability for solar cell applications but also to bring to light new phenomena relevant to other technological applications such as light emitting diodes, lasers,[10,11] optoelectronics,[11] spintronics,[12] and thermoelectrics,[13,14] among others.

In this Perspective, we first outline some unique properties of OMHPs that are critical for PV applications but still not adequately explained. A deeper understanding of these properties will help the development of rational design principles and engineering strategies for performance optimization of OMHPs, as well as the discovery of OMHP-like materials with target functionalities. Here, we identify the key challenges that hinder the wide application of OMHPs, focusing on material stability and I−V hysteresis. We will discuss various material innovation strategies for improving the performance of OMHPs and other potential applications beyond PV. This Perspective concludes with suggestions for new directions and approaches that could lead to new OMHPs with enhanced PCE and stability.

Defect Tolerance. Defects in semiconductors that generate deep gap states (near the middle of the band gap) are known to play an important role in carrier scattering and nonradiative recombination. First-principles calculations have been used to study various point defects (vacancies, interstitials, and antisite substitutions) in lead halide perovskites.[15−20] The results show

Received: August 20, 2015
Accepted: November 12, 2015
Published: November 24, 2015

DOI: 10.1021/acs.jpclett.5b01830
J. Phys. Chem. Lett. 2015, 6, 4862−4872

that these materials exhibit remarkable defect properties because point defects creating deep gap states have high formation energies, whereas those with lower formation energies only create shallow donor and acceptor levels. Furthermore, electron beam-induced current (EBIC) imaging of $MAPbI_{3-x}Cl_x$ shows a uniform distribution of charge extraction efficiency throughout the film, indicating that structural defects such as grain boundaries (GBs) are electrically inert for charge separation and recombination.[21] DFT calculations show that Σ 5(310) GBs (with the grain boundary at the (310) plane and the misorientation angle between two adjoining grains of 36.87°) in $MAPbI_3$ do not generate any states in the gap and, therefore, will not significantly influence the bulk electronic properties.[22] These special defect properties are attributed to the strong antibonding between Pb lone pair s and halogen p, the ionic characteristics, and the large lattice constants.[22,23] First-principles calculations show that the valence band (VB) in pristine $MAPbI_3$ mainly consists of I p orbital character with small components of Pb s orbital character, whereas the conduction band (CB) mainly consists of Pb p orbital character. Due to the strong Pb-s−I-p antibonding coupling, the valence band maximum (VBM) is higher than the I p atomic orbitals. Additionally, because of the weak covalent coupling between Pb p and I p (due to the ionic character of Pb−I bond and large lattice constant), the conduction band minimum (CBM) is not significantly higher than the Pb atomic p states. Consequently, the defect states that are derived from Pb or I atomic states (e.g., Pb and I vacancies) should be close to band extrema, yielding shallow levels. It is noted that the interstitial defects can create deep levels.[22,23] However, the role of the organic cations in defect tolerance is still mostly unknown (besides serving as a large *A*-site cation to maintain the perovskite structure).

The migration of charged defects has been suggested, based on impedance spectroscopy measurements[24] and switchable photocurrent effects.[25] Migration is suggested to be highly relevant for *I*−*V* hysteresis,[26−28] giant low-frequency dielectric constant,[29] self-healing,[30] chemical charge storage,[31] and material stability. Yang et al. demonstrated recently that $MAPbI_3$ has higher ionic conductivity than electronic conductivity due to the diffusion of I^-.[32] The observed room temperature lattice migration of the large I^- anion is likely responsible for both the giant dielectric constant measured at low frequencies as well as the hysteresis in the cyclic sweep experiments. A recent first-principles study of hydrogen migration in $MAPbI_3$ highlights the structural flexibility of hybrid perovskites which enables proton diffusion with low migration barrier via collective iodide displacements, suggesting mobile hydrogenic interstitial impurities under device-relevant conditions.[33] Moreover, ion migration (forming interstitial defects) could create deep charge trapping states,[34] which can strongly affect the performance of OMHP solar cells. Recent computational studies revealed that iodide vacancies and interstitials can easily migrate,[35,36] and cation molecules can also move under bias voltage.[37] Thus, including the effect of ion and defect diffusion is important for guided performance optimization and material innovation via doping.

Ferroelectric Domains and Domain Walls. The presence of ferroelectricity in OMHPs remains elusive. Using first-principles calculations, Frost et al. predicted a large polarization value of 38 $\mu C/cm^2$ for $MAPbI_3$ with PBEsol,[38] whereas Fan et al. reported a polarization of ≈8 $\mu C/cm^2$ for the most stable tetragonal structure,[39] and Zheng et al. found that an antiferroelectric (AFE) tetragonal structure with nearly zero polarization was more stable than its ferroelectric counterpart.[40] Recent DFT investigations from Stroppa et al. reported a polarization of 4.42 $\mu C/cm^2$ for the globally stable tetragonal structure, whereas a structure with AFE alignment is close in energy within room temperature thermal scale.[41]

Thus, including the effect of ion and defect diffusion is important for guided performance optimization and material innovation via doping.

Experimentally, the possible contributions from trapping and detrapping charge carriers,[28,42] ion migration,[24,25,32] and large leakage currents complicate the interpretation of hysteresis loops obtained from macroscopic measurements such as current−voltage (*I*−*V*)[26−28] and polarization−electric field (*P*−*E*) loops.[8,43] Microscopic determination of ferroelectric domains in $MAPbI_3$ with piezoresponse force microscopy (PFM) is complex due to the presence of various surface phenomena, such as electrochemical effects (promoted by humidity),[44] charge accumulation, and surface morphology. Kutes et al. reported direct observations of ferroelectric domains in $MAPbI_3$ with PFM,[45] whereas Xiao et al. and Fan et al. reported the absence of ferroelectricity at room temperature.[25,39] Coll et al. obtained piezo-phase loops for $MAPbI_3$ films with PFM, demonstrating that $MAPbI_3$ has large polarizability but poor polarization retention.[46] They found that the coercivity decays in the time scale of seconds, indicating that $MAPbI_3$ is not ferroelectric at room temperature. On the other hand, Kim et al. reported spontaneous polarization in the absence of electric field for $MAPbI_3$ with PFM, and polarization retention was longer (>60 min) in larger crystals (700 nm length) than smaller ones (400 and 100 nm).[47] These inconsistent observations are attributed to the differences in scan voltage and rate,[46] crystal size and morphology,[47] and defect levels.

Full structural determination of $MAPbI_3$ single crystals, in particularly the orientational order of MA^+ cation, has been the focus of several experimental[48−50] and theoretical works.[51−54] Weller et al. characterized the structures of $MAPbI_3$ with neutron powder diffraction and found that the MA^+ cation at room temperature exhibits a high level of orientational motion, adopting four possible orientations along [100].[49] Several theoretical investigations with ab initio molecular dynamics (MD) suggested that the presence of a strong hydrogen bond network keeps the organic cations oriented along specific directions in the tetragonal phase.[52,54] However, limited by the computational cost, the length and time scales explored in ab initio MD may not be sufficient to capture the relevant dynamics of the organic cations.[51−54] Recent quasielastic neutron scattering measurements combined with Monte Carlo simulations suggested that MA^+ may form AFE or ferroelectric domains.[55] These observations indicate that $MAPbI_3$ at room temperature, even if it does not possess robust ferroelectricity, is still likely to exhibit voltage-induced local polarization caused by the hindered rotation of molecular dipoles.[46]

The presence of polar domains will result in internal electric fields that aid electron−hole separation.[38,56,57] The domain walls, defined as the interfaces separating domains with different polarities, are suggested to serve as separated channels

DOI: 10.1021/acs.jpclett.5b01830
J. Phys. Chem. Lett. 2015, 6, 4862−4872

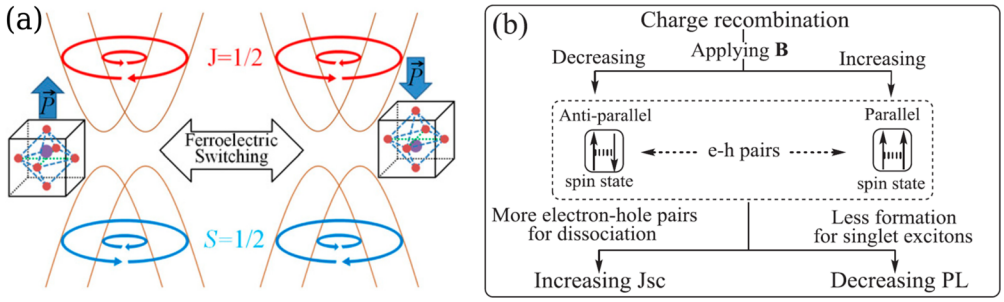

Figure 1. Spin dynamical properties in OMHPs. (a) Schematic illustration of switchable Rashba effect by flipping the molecular dipole direction. Rashba SOC splits the originally degenerate spin-up and spin-down bands. In this case, the spin states in momentum space form "vortex" spin textures (oriented loops in the diagram) with opposite spin rotation directions for inner bands and outer bands, coupled with polar direction. By switching the polarization direction, the spin textures can be flipped for conduction and valence bands. $J = 1/2$ indicates the fully spin−orbital-entangled subspace stemming from intraorbital and interorbital terms. $S = 1/2$ only consists of interorbital term. Reprinted from ref 65. Copyright 2015 National Academy of Sciences. (b) Diagram to show how applied magnetic field affects e−h pairs and gives rise to different photocurrent and magneto-photoluminescence. e−h pairs with parallel spin state are preferably formed under applied magnetic field. Hence, the number of singlet excitations that can recombine radiatively generating photoluminescence signals is reduced, resulting in enhanced photocurrents. Reproduced with permission from ref 68. Copyright 2015 Wiley-VCH Verlag GmbH & Co. KGaA, Weinheim.

for the motions of electrons and holes, thereby preventing recombination.[56] However, the dynamics of domains and domain walls, their relationship with the rotational dynamics of the MA^+ cations,[58,59] and their influence on charge separation remain open questions.[52]

Spin Dynamics and Magnetic Field. One highly interesting feature of $MAPbI_3$ is its juxtaposition of *A* site polar molecules that break inversion symmetry with heavy atoms that bring SOC. SOC must be included to correctly describe the electronic structures of both lead and tin OMHPs.[40,60−64] When inversion symmetry is broken and strong SOC is present, a strong Rashba effect can be observed, and this has been shown in $MAPbI_3$.[41,65,66] The Rashba Hamiltonian is shown in eq 1

$$H_R = \frac{\hbar^2 k^2}{2m} + \hbar\alpha_R \hat{z} \times \vec{k}\cdot\vec{\sigma} \quad (1)$$

where $\vec{\sigma}$ is the Pauli matrices coupled with wavevector $\vec{k}$, and α_R indicates the Rashba SOC strength. In this case, the originally degenerate spin-up and spin-down bands are lifted, creating helical spin textures in momentum space. By applying an external electric field to control the orientation of molecular dipole moments, the spin helicity can be switched (Figure 1a).[65] However, the study of the Rashba effect is still limited to ground state properties. Its possible role in promoting the high carrier mobility and long lifetime in OMHPs has been proposed theoretically and merits further experimental investigation.[67] The magneto-photoluminescence and photocurrent were measured under magnetic field.[68,69] It was found that by changing the spin state of electron−hole pairs from singlet to triplet via magnetic field, they have lower probability to form excitons and recombine radiatively, thus giving rise to higher photocurrent as shown in Figure 1b. Multiferroics that couple polarization and magnetization have drawn intensive investigations for their promising device applications. Magnetic ordering has not been observed in $MAPbI_3$, but by inserting magnetic ions as defects or solid solutions, this material may simultaneously present ferroelectricity, magnetization and SOC, offering a great platform to study the interplay of these phenomena and to open additional potential applications. Furthermore, Giovanni et al. reported using polarized light to probe the spin relaxation time in $MAPbI_3$, showing that the electron spin-relaxation time scale is approximately 10 ps, and holes have faster relaxation (≈ 1 ps).[12] The Elliot−Yafet mechanism is believed to be the dominant source of spin relaxation, in which the spin of carriers is flipped mainly due to impurities and grain boundaries. This illustrates potential role of $MAPbI_3$ as a new candidate for ultrafast spintronics applications.

Beyond Photovoltaic. Further functionality is proposed, as lead- and tin-based OMHPs have been considered for thermoelectric applications because of their large Seebeck coefficient[8,70,71] and low thermal conductivity.[72] On the basis of first-principles modeling, He and Galli proposed that the thermoelectric figure of merit (ZT) for $MAPbI_3$ and $MASnI_3$ may reach values of 1 to 2 by suitable doping to increase carrier density.[13] Experimental investigations found that both $MAPbI_3$ and $MASnI_3$ show very low ZT in pristine form, though chemical doping of $MASnI_3$ enhances its ZT by 3 orders of magnitude, reaching 0.13 at room temperature.[14] It remains a challenge to make these materials attractive for thermoelectric applications ($ZT = 3$).[14,73] In addition, OMHPs are recently introduced as new materials for nanolasers due to their high fluorescence yields and wavelength tunability.[74−77] The lasing performance in lead halide films[74] and nanoplates[78] was not optimal because of their high threshold carrier density required for lasing. Zhu et al. synthesized single-crystal OMHP nanowires realizing room-temperature and wavelength-tunable lasing with very low thresholds (220 nJ cm^{-2}) and high quality factors ($Q \approx 3600$).[11] These findings highlight the potential applications of OMHPs to miniaturized lasers. However, as also illustrated in ref 11, under continuous laser irradiation, the material degrades over a few tens of minutes. Investigating and improving the stability of OMHPs have become critical challenges.

Further functionality is proposed, as lead- and tin-based OMHPs have been considered for thermoelectric applications because of their large Seebeck coefficient.

Stability Challenges. Strategies to prolong the stability of OMHPs must be developed to enable the commercialization of its novel applications. Their low stability includes degradation upon exposure to moisture, light, or heat.[79−81] Initial strategies

DOI: 10.1021/acs.jpclett.5b01830
J. Phys. Chem. Lett. 2015, 6, 4862−4872

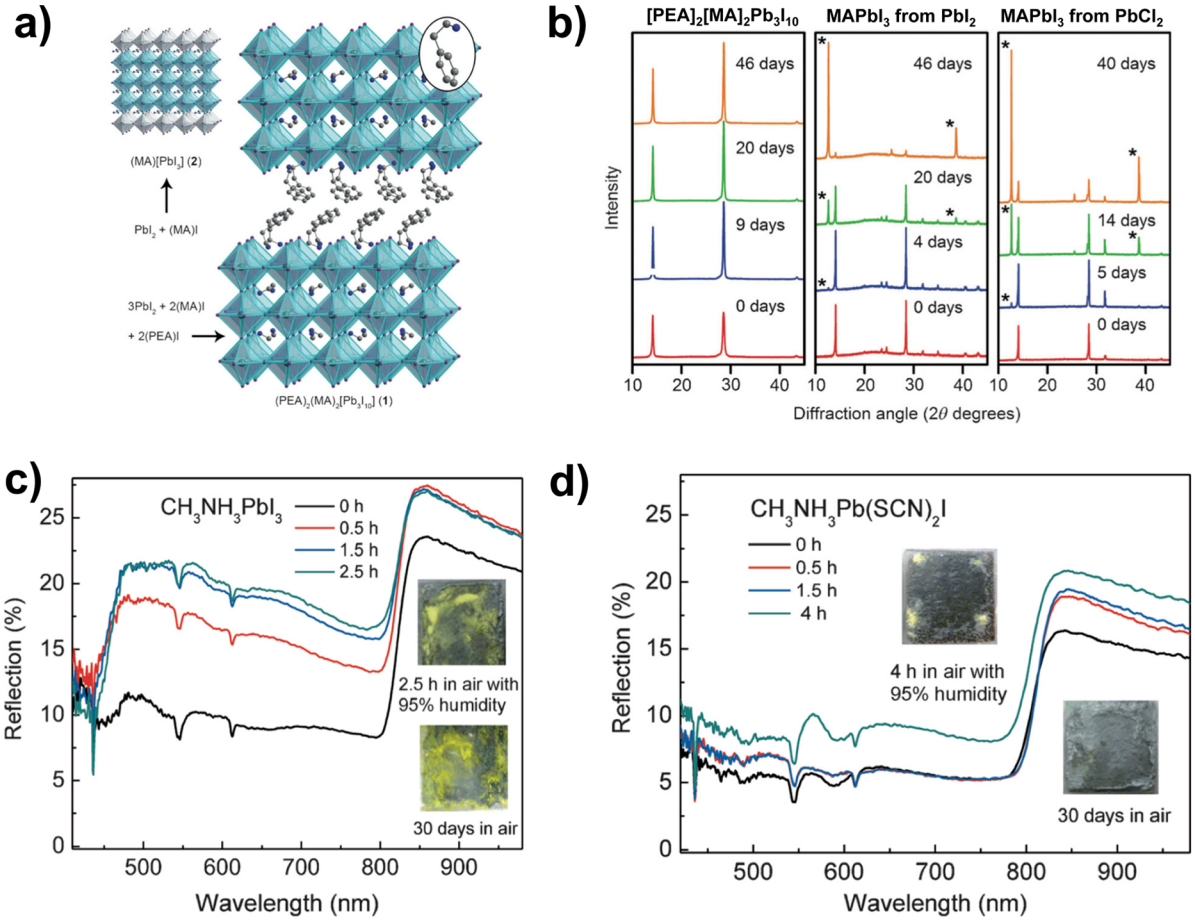

Figure 2. Enhancement in structural stability via material innovation. (a) Atomic structure of the $[PEA]_2[MA]_2Pb_3I_{10}$ 2D hybrid perovskite proposed to enhance the lifetime. (b) Powder X-ray diffraction comparing the presence of PbI_2 residue in $[PEA]_2[MA]_2Pb_3I_{10}$, in $MAPbI_3$ formed from PbI_2, and in $MAPbI_3$ formed from $PbCl_2$ after more than 40 days exposed to 52% humidity. Reproduced with permission from ref 91. Copyright 2015 Wiley-VCH Verlag GmbH & Co. KGaA, Weinheim. (c) Reflectivity measurements of $MAPbI_3$ films after accelerated exposure to 95% humidity; inset image shows advanced degradation after 30 days. (d) Reflectivity measurements of $MAPb(SCN)_2I$ films after accelerated exposure to 95% humidity; inset image shows no significant degradation after 30 days. Reproduced with permission from ref 92. Copyright 2015 Wiley-VCH Verlag GmbH & Co. KGaA, Weinheim.

against moisture include encapsulation of the film with hydrophobic materials to enhance its stability.[82] However, moving toward a better understanding of the mechanisms of degradation could enable material design and engineering schemes to achieve long-term stability. New material design tools can focus on increasing the hydrophobicity of the material to prevent the formation of a hydrate state, which is considered to be the initial stage of the degradation mechanism.

New material design tools can focus on increasing the hydrophobicity of the material to prevent the formation of a hydrate state, which is considered to be the initial stage of the degradation mechanism.

The initial stage of the degradation process starts with surface of the material interacting with its environment. To date, the thermodynamically stable terminations of the tetragonal[83] and orthorhombic[84] $MAPbI_3$ surfaces have been studied theoretically, but the degradation mechanism is still an open question. One proposed mechanism is that MAI and PbI_2 can be generated within the material leading to further breakdown to CH_3NH_2 and HI, concluding with I_2(solid) and H_2(gas) after exposure to oxygen and sunlight.[81,85] Additionally, a recent work explores MA fragmentation as part of the degradation process.[30] It has also been suggested that water undergoes an acid–base reaction with the MA^+ cation, leading to HI, CH_3NH_2, H_2O, and PbI_2.[38] The initial steps of the degradation process have been studied in more depth. Leguy et al. observed that $MAPbI_3$ responds differently to moisture, depending on the concentration.[86] A transparent monohydrate ($MAPbI_3{\cdot}H_2O$) is formed at low humidity, which can be dehydrated back to $MAPbI_3$ by raising the temperature. However, if the system is further exposed to water vapor, the monohydrate converts to a dihydrate ($[MA]_4PbI_6{\cdot}2H_2O$), which eventually irreversibly decomposes.[80,86] Interestingly, the idea of water penetrating into OMHPs along grain boundaries has also been proposed.[86] Both Christians et al. and Yang et al. found that hydrate states are formed in the system[87,88] with at least partial recovery of the perovskite when the system is dehydrated. Illumination plays a significant role in the recovery process, as it was reported that the perovskite decomposes differently in dark and light conditions.[87] Moisture and illumination cause the perovskite to degrade to PbI_2, but in the dark, PbI_2 is not formed. Additionally, recent theoretical

DOI: 10.1021/acs.jpclett.5b01830
J. Phys. Chem. Lett. 2015, 6, 4862−4872

studies reported results from ab initio molecular dynamics[89] and first-principles calculations[90] of $MAPbI_3$ in contact with liquid water environment, suggesting that PbI_2-terminated surfaces are resistant to water and that the MA dipole direction plays a role in the energetics of water penetration inside the material.

Although detailed understanding of the degradation mechanism remains an active research area, material design efforts have recently yielded progress in enhancing the stability of films. One promising approach in the design of new materials is the modulation of the phase dimensionality of the inorganic framework and the organic component. Recently, the 2D hybrid perovskite $[PEA]_2[MA]_2Pb_3I_{10}$, where $[PEA] = C_6H_5(CH_2)_2NH_3$, has been proposed and synthesized. It exhibits high quality films with greater resistance to moisture than $MAPbI_3$ (formed from either PbI_2 and $PbCl_2$[91]), as shown in Figure 2a and b. This approach gives 2D hybrid perovskite films without signs of degradation even after more than 40 days. Another material design approach, which relies on anion substitutions, has recently led to significant stability as the film is exposed to high levels of humidity,[92] as shown in Figure 2c and d. In this specific case, SCN^- anions are substituted for iodide ions in $MAPbI_3$ while maintaining a competitive PCE. These results hint at the benefits of complementing current stability enhancement efforts such as interfacial engineering,[93] encapsulation,[94,95] and improved fabrication techniques[96] with material design tools to drive new breakthroughs in OMHP stability. New material design tools can focus on increasing the hydrophobicity of the material to prevent the formation of a hydrate state, which is considered to be the initial stage of the degradation mechanism.

Hysteresis and Optical Effects. In addition to the stability challenges, another serious concern before market viability is the optimization of the PCE value, which is extracted from current−voltage (I−V) curves. The determination of the PCE of OMHP-based solar cells is somewhat ambiguous, as the measured I−V is found to depend on the fabrication/age of the sample,[26,97−101] the scanning direction, and the rate of voltage change.[28,98,99,102,103] Although the origin is still unclear, the observed anomalous I−V hysteresis is due to multiple factors occurring concurrently, either independently or coupled. It is suggested that the interfaces between the OMHP absorber and the electron/hole transporters contain defect states, where carriers will be trapped differently depending on the voltage scanning direction and rate.[26,28,98,102,104,105] Wu et al. show that these trap states can result from electron−phonon coupling even at the defect-free interfaces and surfaces.[106] Interface engineering that reduces trap states, such as modifying electron transporter TiO_2 with a C_{60} self-assembled monolayer, has proven to be an efficient way to suppress the hysteresis.[107−109] Abate et al. use the supramolecular (iodopentafluorobenzene) halogen bonds to passivate the undercoordinated I site, which is shown to reduce trap sites near the perovskite surface.[110] Fabricating a prototype cell with a mesoporous TiO_2 layer, incorporating Zr into TiO_2 electrodes, and treating the interface with pyridine are all demonstrated to reduce hysteresis and increase the PCE.[98,111] Similarly, OMHPs with large grains are found to give rise to hysteresis-free I−V curves,[47,100,112] as the large grains can effectively reduce the number of trap states in the grain boundaries. In addition, the aforementioned ferroelectric response originating from permanent molecular dipole moments is also suggested to play an important role in I−V hysteresis.[8,43,45,54,99,100] In particular, shift current as the main mechanism of the bulk PV effect may produce photocurrent and contribute to the measured hysteresis.[113,114] Because shift current emerges in systems lacking inversion symmetry, the magnitude of shift current will be larger when all the molecular dipoles aligned in parallel.[40] Moreover, as raised by Dualeh et al., ion migration can also cause the I−V hysteresis.[24,28,97] This is further supported by the change in X-ray diffraction peaks, which suggests a reversible photoinduced ion migration.[115] The bulk properties of OMHPs become quite different under light illumination. For example, substantial enhancement of the dielectric and piezoelectric responses are observed with light illumination.[29,46] Wu et al. found a photoinduced change of dipole moments using a modulation electroabsorption spectroscopy method.[116] Additionally, a theoretical work indicates that the molecules can rotate more easily under excitation because of the charge transfer from I to Pb.[117] This may also be related to various hysteresis observations. These findings illustrate that the structural and electronic properties of OMHPs after light absorption may deviate from their ground-state properties significantly. More subtly, the phonon vibrations can be strongly affected by excitation and high concentrations of free carriers. Therefore, understanding the dynamics of the excited state is significant to understand the properties and provide further guidelines to enhance the device performance.

Material Design Innovation. Besides the solar cell application, the OMHP architecture has become a promising platform for the design and optimization of functional materials. These design schemes aim to leverage on the material's defect tolerance while improving hysteresis, stability, and further functionality. This crystal architecture, consisting of ABX_3 (organic monovalent cation, A; divalent metal, B; and inorganic or organic anion, X), provides a tremendous capacity to tune the structural, electronic, optical, and magnetic properties to achieve a variety of target functionalities. To achieve this, The current theoretical and experimental material design efforts have exploited the structural flexibility of these materials at different size scales by varying atomic compositions, modulating phase dimensionality, and controlling nanoscale particle shape.

The current theoretical and experimental material design efforts have exploited the structural flexibility of these materials at different size scales by varying atomic compositions, modulating phase dimensionality, and controlling nanoscale particle shape.

Substituting ABX_3 atomic constituents guides the structure−property−function framework and contributes to the understanding of $MAPbI_3$ performance and stability. This design scheme should comply with Goldschmidt's tolerance factor (t),[118] which was recently adapted for sulfide perovskites[119−121] and organic−inorganic perovskites.[122,123] Kieslich et al. reported t for hybrid perovskites by treating all ions as hard spheres or cylinders taking into consideration the molecular free rotation around its center of mass to deduce effective ionic radii for organic ions.[122] The t values for all the possible ABX_3 combinations accounting for ionic charge based on the lists shown in Figure 3a were computed, suggesting that 742 of the resulting compounds could form a cubic perovskite phase, since they have tolerance factors of ≈0.8−1.0.[123] Only 140 of these are known

DOI: 10.1021/acs.jpclett.5b01830
J. Phys. Chem. Lett. 2015, 6, 4862−4872

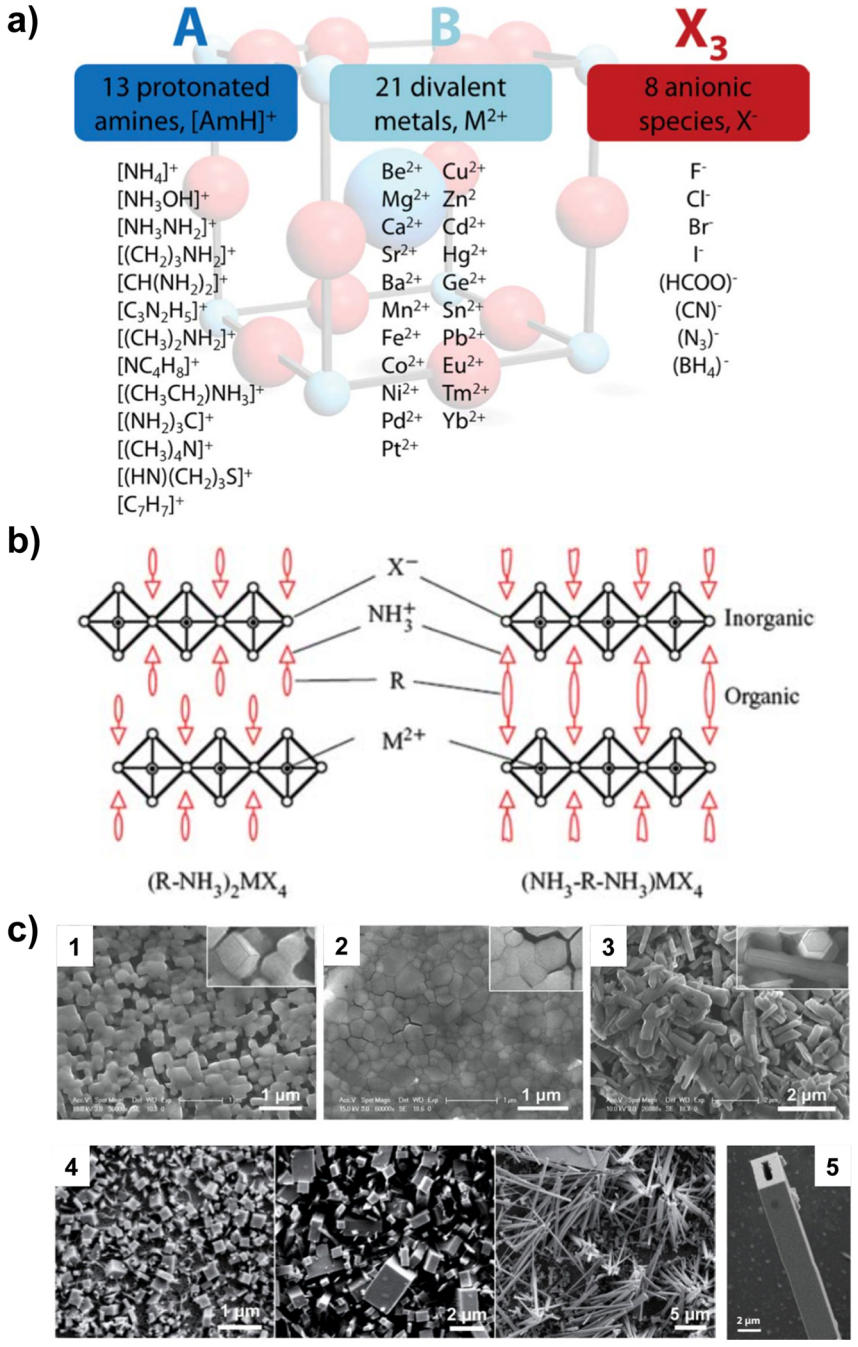

Figure 3. Material design strategies from atomic manipulation to nanoscale particle shape. (a) Recently proposed combinations of A = organic cation, B = metal cation, and X = organic or inorganic anion. The approach of this study was to systematically permute 13 protonated amines (Note: this list includes a nonamine system, tropylium, $C_7H_7^+$), 21 divalent metal ions, and 8 anionic species to compute the tolerance factor (t) of 2184 structures, identifying which ones are within the stability range of perovskite cubic and related structures. This initial survey does not account for the electronic structure and the nature of the bonding character. Reprinted from ref 123. Copyright 2015 Royal Society of Chemistry. (b) Schematic of the atomic structure of the 2D layered hybrid perovskite. The $(R{-}NH_3)_2MX_4$ structure is analogous to Ruddlesden−Popper phases, whereas the $(NH_3{-}R{-}NH_3)_2MX_4$ structure is analogous to layered perovskites, where the quasi-2D perovskite layers are separated by long organic chains. Reprinted from ref 144. Copyright 2010 Royal Society of Chemistry. (c) Scanning electron microscopy images of $MAPbI_3$ as (1) cubic nanoparticle, (2) hexagonal nanoparticle, and (3) nanorods. Reprinted from ref 151. Copyright 2014 IOP Publishing Ltd. Scanning electron microscopy images of $MAPbCl_3$ as (4) a function of time [1 min, 30 min, and 15 h] and (5) nanotubes. Reprinted from ref 11. Copyright 2015 Nature Publishing Group.

materials, leaving an extensive number of not-yet-explored OMHPs. This approach does not account for the bonding character of the constituents in the predicted materials, suggesting the exploration of alternative design schemes.

The discovery of new materials can be achieved by tailoring the atomic structure of known hybrid perovskites. Explicitly modifying the A-site organic cation has led to improved structural stability of the $MAPbI_3$-based solar cell. For example, $[HC(NH_2)_2]PbI_3$, where $HC(NH_2)_2^+$ is formamidium, shows thermal stability advantages, as it does not undergo a phase transition around operating temperatures;[124] however, the initially reported PCE is not competitive.[125] An improvement

DOI: 10.1021/acs.jpclett.5b01830
J. Phys. Chem. Lett. 2015, 6, 4862−4872

in the PCE was achieved in mixed-organic-cation systems, $[MA]_{0.6}[HC(NH_2)_2]_{0.4}PbI_3$.[126] A theoretical approach to replace the MA^+ cation with a zero-dipole organic cation, $C(NH_2)_3^+$, was proposed, with the objective of reducing $I-V$ hysteresis in $MAPbI_3$ while maintaining the electronic properties.[127] In order to produce lead-free hybrid perovskites, researchers have modulated the B site with two main candidates, Ge and Sn.[128−130] Polar Ge-based hybrid perovskites with multiple A-site organic cations were successfully synthesized very recently,[131] exhibiting large second harmonic generation response. In the case of $MASnI_3$, the electrical properties are promising; however, Sn^{2+} is easily oxidized to Sn^{4+}, leading to poor stability.[132,133] Enhanced properties can be obtained by doping the material with Pb, $MAPb_{1-x}Sn_xI_3$, as it has been reported experimentally and theoretically[134,135] to slow down the Sn oxidation. Mixing Cl onto the X-site yields even better stability for both Sn- and Pb-based OMHPs,[136] although the role of Cl is still not explained. It has been reported that the inclusion of Cl into $MAPbI_3$ generates improved film morphology[137] and more uniform films.[138] These efforts have provided key insights to tackle the performance and stability challenges of the hybrid perovskite solar cell.

The crystal phase dimensionality and composition of the hybrid perovskite can be varied by incorporating either a small radius divalent metal or a long organic cation chain suggesting many additional inventive directions, as illustrated in Figure 3a, that could further enhance the functionality of these materials. For instance, small radius transition metals, such as Mn^{2+}, Fe^{2+}, Co^{2+}, Ni^{2+}, can be used to design new multifunctional OMHPs, which could extend to other crystal phases. These modifications could enable the presence of functional electronic, optical, and magnetic properties within the hybrid perovskite material as is the case for $(RNH_3)_2FeX_4$, where R = CH_3, C_2H_5, C_3H_7, and $C_6H_5CH_2$ and X = Cl, Br.[139,140] This structure is analogous to the inorganic Ruddlesden−Popper phase. The magnetic properties of this family of materials has been studied, finding a canted spin system as its magnetic ground state,[141,142] but no further study on how magnetism couples with optical or electrical properties has been reported. Another material that has been realized is $[MA]_2CuX_4$, with X = Cl, Br, or an alloy of both, yielding promising electronic properties.[143] As shown in Figure 3b, these materials have a 2D layered structure where the layers of BX_6 octahedra are separated by layers of organic molecules,[144] leading to flexible mechanical properties and useful light emission.[145,146] Another material that was recently introduced is Cs_2SnI_6; its unique electronic and optical properties make it a promising candidate for the basis of new high-efficiency, lead-free solar cells.[147] Additionally, this design strategy has also advanced the understanding of the structural stability for the hybrid perovskite solar cell, as a 2D hybrid perovskite of the form $[PEA]_2[MA]_2Pb_3I_{10}$ has shown higher resistance to moisture[91] potentially due to the hydrophobicity of the benzene ring.

The ability to synthesize OMHP nanostructures represents a significant step forward on the quest for novel applications. Nanoparticles of $MAPbBr_3$ have demonstrated remarkable optical properties and functionalities as quantum dot solar cells.[148,149] Additionally, these nanoparticles showed high selectivity and sensitivity for detection of acidic phenols, specifically picric acid.[150] The control of nanocrystal shapes has been achieved, as shown in Figure 3c, including (1) cubic and (2) hexagonal nanoparticles, (3) nanorods, (4) nanowires, and (5) nanotubes. These efforts led to the observation of new phenomena with technological relevance such as nano-optoelectronic devices[151] and lasing.[11]

In summary, OMHPs with exceptional properties, such as ferroelectricity, long carrier lifetime, and strong SOC, provide a great deal of opportunities not only in photovoltaics but also in a wide range of potential applications including thermal power and optics. Understanding these properties is essential to the design of new sets of materials for specific applications. However, the challenges raised by extending the chemical stability and reducing the I/V hysteresis must be overcome to unlock their potential. Material innovation has been demonstrated to be an effective way to strengthen the chemical stability and optimize energy conversion, which are central and active topics in the OMHPs field. Exploring compositional and structural variations within this perovskite family is a promising way of optimizing OMHP performance, and it can also inspire ideas to transplant these valuable properties into other material families for applications of technological relevance.

AUTHOR INFORMATION

Corresponding Author

*E-mail: rappe@sas.upenn.edu.

Notes

The authors declare no competing financial interest.

Biographies

Fan Zheng received his B.Sc. degree from the University of Science and Technology of China in 2010. He is currently a Ph.D. student in Physical Chemistry at the University of Pennsylvania.

Diomedes Saldana-Greco is a Ph.D. candidate in Physical Chemistry at the University of Pennsylvania. He received his B.Sc. cum laude in Chemistry with Honors and a Minor in Mathematics from the University of Richmond in 2010.

Shi Liu joined Geophysical Laboratory, Carnegie Institution for Science, on the first of September in 2015 as a Carnegie Fellow. He received his B.S. from University of Science and Technology of China in 2009 and his Ph.D. from University of Pennsylvania in 2015. His research interests include multiscale simulations of ferroelectrics, solar materials, and free radical polymerization.

Andrew M. Rappe is Professor of Chemistry and Professor of Materials Science and Engineering at the University of Pennsylvania. He received his A.B. summa cum laude from Harvard University in 1986, and his Ph. D. from MIT in 1992. He was an IBM Postdoctoral Fellow at UC Berkeley 1992−1994. http://www.sas.upenn.edu/rappegroup/.

ACKNOWLEDGMENTS

F.Z. was supported by the Department of Energy Office of Basic Energy Sciences under Grant Number DE-FG02-07ER46431. D.S.G. was supported by the U.S. Department of Energy Office of Basic Energy Sciences under Grant No. DE-FG02-07ER15920. S.L. was supported by the NSF under Grant DMR-1124696 and the Carnegie Institution for Science. A.M.R. was supported by the Office of Naval Research under Grant N00014-14-1-0761.

REFERENCES

(1) NREL. Research Cell Efficiency Records. http://www.nrel.gov/ncpv/images/efficiency_chart.jpg (accessed October, 2015).

(2) Kojima, A.; Teshima, K.; Shirai, Y.; Miyasaka, T. Organometal Halide Perovskites As Visible-Light Sensitizers for Photovoltaic Cells. *J. Am. Chem. Soc.* **2009**, *131*, 6050−6051.

DOI: 10.1021/acs.jpclett.5b01830
J. Phys. Chem. Lett. 2015, 6, 4862−4872

(3) Baikie, T.; Fang, Y.; Kadro, J. M.; Schreyer, M.; Wei, F.; Mhaisalkar, S. G.; Graetzel, M.; White, T. J. Synthesis and Crystal Chemistry of the Hybrid Perovskite $(CH_3NH_3)PbI_3$ for Solid-State Sensitised Solar Cell Applications. *J. Mater. Chem. A* **2013**, *1*, 5628−5641.
(4) Im, J.-H.; Lee, C.-R.; Lee, J.-W.; Park, S.-W.; Park, N.-G. 6.5% Efficient Perovskite Quantum-Dot-Sensitized Solar Cell. *Nanoscale* **2011**, *3*, 4088−4093.
(5) Filip, M. R.; Eperon, G. E.; Snaith, H. J.; Giustino, F. Steric Engineering of Metal-Halide Perovskites with Tunable Optical Band Gaps. *Nat. Commun.* **2014**, *5*, 5757−9.
(6) Lee, M. M.; Teuscher, J.; Miyasaka, T.; Murakami, T. N.; Snaith, H. J. Efficient Hybrid Solar Cells Based on Meso-Superstructured Organometal Halide Perovskites. *Science* **2012**, *338*, 643−647.
(7) Etgar, L.; Gao, P.; Xue, Z.; Peng, Q.; Chandiran, A. K.; Liu, B.; Nazeeruddin, M. K.; Graetzel, M. Mesoscopic $CH_3NH_3PbI_3/TiO_2$ Heterojunction Solar Cells. *J. Am. Chem. Soc.* **2012**, *134*, 17396−17399.
(8) Stoumpos, C. C.; Malliakas, C. D.; Kanatzidis, M. G. Semiconducting Tin and Lead Iodide Perovskites with Organic Cations: Phase Transitions, High Mobilities, and Near-Infrared Photoluminescent Properties. *Inorg. Chem.* **2013**, *52*, 9019−9038.
(9) Berry, J.; Buonassisi, T.; Egger, D. A.; Hodes, G.; Kronik, L.; Loo, Y.-L.; Lubomirsky, I.; Marder, S. R.; Matsai, Y.; Miller, J. S.; et al. Hybrid Organic-Inorganic Perosvkites (HOIPs): Opportunities and Challenges. *Adv. Mater.* **2015**, *27*, 5102−5112.
(10) Fu, A.; Yang, P. Organic-Inorganic Perovskites: Lower Threshold for Nanowire Lasers. *Nat. Mater.* **2015**, *14*, 557−558.
(11) Zhu, H.; Fu, Y.; Meng, F.; Wu, X.; Gong, Z.; Ding, Q.; Gustafsson, M. V.; Trinh, M. T.; Jin, S.; Zhu, X.-Y. Lead halide Perovskite Nanowire Lasers with Low Lasing Thresholds and High Quality Factors. *Nat. Mater.* **2015**, *14*, 636−642.
(12) Giovanni, D.; Ma, H.; Chua, J.; Grätzel, M.; Ramesh, R.; Mhaisalkar, S.; Mathews, N.; Sum, T. C. Highly Spin-Polarized Carrier Dynamics and Ultralarge Photoinduced Magnetization in $CH_3NH_3PbI_3$ Perovskite Thin Films. *Nano Lett.* **2015**, *15*, 1553−1558.
(13) He, Y.; Galli, G. Perovskites for Solar Thermoelectric Applications: A First Principle Study of $CH_3NH_3AI_3$ (A = Pb and Sn). *Chem. Mater.* **2014**, *26*, 5394−5400.
(14) Mettan, X.; Pisoni, R.; Matus, P.; Pisoni, A.; Jaćimović, J.; Náfrádi, B.; Spina, M.; Pavuna, D.; Forró, L.; Horváth, E. Tuning of the Thermoelectric Figure of Merit of $CH_3NH_3MI_3$ (M = Pb, Sn) Photovoltaic Perovskites. *J. Phys. Chem. C* **2015**, *119*, 11506−11510.
(15) Yin, W.-J.; Shi, T.; Yan, Y. Unique Properties of Halide Perovskites As Possible Origins of the Superior Solar Cell Performance. *Adv. Mater.* **2014**, *26*, 4653−4658.
(16) Yin, W.-J.; Shi, T.; Yan, Y. Unusual Defect Physics in $CH_3NH_3PbI_3$ Perovskite Solar Cell Absorber. *Appl. Phys. Lett.* **2014**, *104*, 063903.
(17) Kim, J.; Lee, S.-H.; Lee, J. H.; Hong, K.-H. The Role of Intrinsic Defects in Methylammonium Lead Iodide Perovskite. *J. Phys. Chem. Lett.* **2014**, *5*, 1312−1317.
(18) Walsh, A.; Scanlon, D. O.; Chen, S.; Gong, X. G.; Wei, S.-H. Self-Regulation Mechanism for Charged Point Defects in Hybrid Halide Perovskites. *Angew. Chem.* **2015**, *127*, 1811−1814.
(19) Buin, A.; Pietsch, P.; Xu, J.; Voznyy, O.; Ip, A. H.; Comin, R.; Sargent, E. H. Materials Processing Routes to Trap-Free Halide Perovskites. *Nano Lett.* **2014**, *14*, 6281−6286.
(20) Shi, T.; Yin, W.-J.; Hong, F.; Zhu, K.; Yan, Y. Unipolar Self-Doping Behavior in Perovskite $CH_3NH_3PbBr_3$. *Appl. Phys. Lett.* **2015**, *106*, 103902.
(21) Edri, E.; Kirmayer, S.; Henning, A.; Mukhopadhyay, S.; Gartsman, K.; Rosenwaks, Y.; Hodes, G.; Cahen, D. Why Lead Methylammonium Tri-Iodide Perovskite-Based Solar Cells Require a Mesoporous Electron Transporting Scaffold (but Not Necessarily a Hole Conductor). *Nano Lett.* **2014**, *14*, 1000−1004.
(22) Yin, W.-J.; Shi, T.; Yan, Y. Superior Photovoltaic Properties of Lead Halide Perovskites: Insights from First-Principles Theory. *J. Phys. Chem. C* **2015**, *119*, 5253−5264.
(23) Yin, W.-J.; Yang, J.-H.; Kang, J.; Yan, Y.; Wei, S.-H. Halide Perovskite Materials for Solar Cells: A Theoretical Review. *J. Mater. Chem. A* **2015**, *3*, 8926−8942.
(24) Dualeh, A.; Moehl, T.; Tetreault, N.; Teuscher, J.; Gao, P.; Nazeeruddin, M. K.; Graetzel, M. Impedance Spectroscopic Analysis of Lead Iodide Perovskite-Sensitized Solid-State Solar Cells. *ACS Nano* **2014**, *8*, 362−373.
(25) Xiao, Z.; Yuan, Y.; Shao, Y.; Wang, Q.; Dong, Q.; Bi, C.; Sharma, P.; Gruverman, A.; Huang, J. Giant Switchable Photovoltaic Effect in Organometal Trihalide Perovskite Devices. *Nat. Mater.* **2014**, *14*, 193−198.
(26) Unger, E. L.; Hoke, E. T.; Bailie, C. D.; Nguyen, W. H.; Bowring, A. R.; Heumüller, T.; Christoforo, M. G.; McGehee, M. D. Hysteresis and Transient Behavior in Current-Voltage Measurements of Hybrid-Perovskite Absorber Solar Cells. *Energy Environ. Sci.* **2014**, *7*, 3690−3698.
(27) Chen, H.-W.; Sakai, N.; Ikegami, M.; Miyasaka, T. Emergence of Hysteresis and Transient Ferroelectric Response in Organo-Lead Halide Perovskite Solar Cells. *J. Phys. Chem. Lett.* **2015**, *6*, 164−169.
(28) Snaith, H. J.; Abate, A.; Ball, J. M.; Eperon, G. E.; Leijtens, T.; Noel, N. K.; Stranks, S. D.; Wang, J. T.-W.; Wojciechowski, K.; Zhang, W. Anomalous Hysteresis in Perovskite Solar Cells. *J. Phys. Chem. Lett.* **2014**, *5*, 1511−1515.
(29) Juarez-Perez, E. J.; Sanchez, R. S.; Badia, L.; Garcia-Belmonte, G.; Kang, Y. S.; Mora-Sero, I.; Bisquert, J. Photoinduced Giant Dielectric Constant in Lead Halide Perovskite Solar Cells. *J. Phys. Chem. Lett.* **2014**, *5*, 2390−2394.
(30) Delugas, P.; Filippetti, A.; Mattoni, A. Methylammonium Fragmentation in Amines As Source of Localized Trap Levels and the Healing Role of Cl in Hybrid Lead-Iodide Perovskites. *Phys. Rev. B: Condens. Matter Mater. Phys.* **2015**, *92*, 045301.
(31) O'Regan, B. C.; Barnes, P. R. F.; Li, X.; Law, C.; Palomares, E.; Marin-Beloqui, J. M. Optoelectronic Studies of Methylammonium Lead Iodide Perovskite Solar Cells with Mesoporous TiO_2: Separation of Electronic and Chemical Charge Storage, Understanding Two Recombination Lifetimes, and the Evolution of Band Offsets During J-V Hysteresis. *J. Am. Chem. Soc.* **2015**, *137*, 5087−5099.
(32) Yang, T.-Y.; Gregori, G.; Pellet, N.; Grätzel, M.; Maier, J. The Significance of Ion Conduction in a Hybrid Organic-Inorganic Lead-Iodide-Based Perovskite Photosensitizer. *Angew. Chem., Int. Ed.* **2015**, *54*, 7905−7910.
(33) Egger, D. A.; Kronik, L.; Rappe, A. M. Theory of Hydrogen Migration in Organic−Inorganic Halide Perovskites. *Angew. Chem., Int. Ed.* **2015**, *54*, 12437.
(34) Du, M. H. Efficient Carrier Transport in Halide Perovskites: Theoretical Perspectives. *J. Mater. Chem. A* **2014**, *2*, 9091−9098.
(35) Azpiroz, J. M.; Mosconi, E.; Bisquert, J.; De Angelis, F. Defect Migration in Methylammonium Lead Iodide and its Role in Perovskite Solar Cell Operation. *Energy Environ. Sci.* **2015**, *8*, 2118−2127.
(36) Eames, C.; Frost, J. M.; Barnes, P. R. F.; O'Regan, B. C.; Walsh, A.; Islam, M. S. Ionic Transport in Hybrid Lead Iodide Perovskite Solar Cells. *Nat. Commun.* **2015**, *6*, 7497.
(37) Haruyama, J.; Sodeyama, K.; Han, L.; Tateyama, Y. First-Principles Study of Ion Diffusion in Perovskite Solar Cell Sensitizers. *J. Am. Chem. Soc.* **2015**, *137*, 10048−10051.
(38) Frost, J. M.; Butler, K. T.; Brivio, F.; Hendon, C. H.; van Schilfgaarde, M.; Walsh, A. Atomistic Origins of High-Performance in Hybrid Halide Perovskite Solar Cells. *Nano Lett.* **2014**, *14*, 2584−2590.
(39) Fan, Z.; Xiao, J.; Sun, K.; Chen, L.; Hu, Y.; Ouyang, J.; Ong, K. P.; Zeng, K.; Wang, J. Ferroelectricity of $CH_3NH_3PbI_3$ Perovskite. *J. Phys. Chem. Lett.* **2015**, *6*, 1155−1161.
(40) Zheng, F.; Takenaka, H.; Wang, F.; Koocher, N. Z.; Rappe, A. M. First-Principles Calculation of Bulk Photovoltaic Effect in $CH_3NH_3PbI_3$ and $CH_3NH_3PbI_{3-x}Cl_x$. *J. Phys. Chem. Lett.* **2015**, *6*, 31−37.
(41) Stroppa, A.; Di Sante, D.; Barone, P.; Bokdam, M.; Kresse, G.; Franchini, C.; Whangbo, M.-H.; Picozzi, S. Tunable Ferroelectric

DOI: 10.1021/acs.jpclett.5b01830
J. Phys. Chem. Lett. 2015, 6, 4862−4872

Polarization and Its Interplay with Spin-Orbit Coupling in Tin Iodide Perovskites. *Nat. Commun.* **2014**, *5*, 5900.
(42) Shao, Y.; Xiao, Z.; Bi, C.; Yuan, Y.; Huang, J. Origin and Elimination of Photocurrent Hysteresis by Fullerene Passivation in $CH_3NH_3PbI_3$ Planar Heterojunction Solar Cells. *Nat. Commun.* **2014**, *5*, 5784.
(43) Wei, J.; Zhao, Y.; Li, H.; Li, G.; Pan, J.; Xu, D.; Zhao, Q.; Yu, D. Hysteresis Analysis Based on the Ferroelectric Effect in Hybrid Perovskite Solar Cells. *J. Phys. Chem. Lett.* **2014**, *5*, 3937−3945.
(44) Dahan, D.; Molotskii, M.; Rosenman, G.; Rosenwaks, Y. Ferroelectric Domain Inversion: The Role of Humidity. *Appl. Phys. Lett.* **2006**, *89*, 152902.
(45) Kutes, Y.; Ye, L.; Zhou, Y.; Pang, S.; Huey, B. D.; Padture, N. P. Direct Observation of Ferroelectric Domains in Solution-Processed $CH_3NH_3PbI_3$ Perovskite Thin Films. *J. Phys. Chem. Lett.* **2014**, *5*, 3335−3339.
(46) Coll, M.; Gomez, A.; Mas-Marza, E.; Almora, O.; Garcia-Belmonte, G.; Campoy-Quiles, M.; Bisquert, J. Polarization Switching and Light-Enhanced Piezoelectricity in Lead Halide Perovskites. *J. Phys. Chem. Lett.* **2015**, *6*, 1408−1413.
(47) Kim, H.-S.; Kim, S. K.; Kim, B. J.; Shin, K.-S.; Gupta, M. K.; Jung, H. S.; Kim, S.-W.; Park, N.-G. Ferroelectric Polarization in $CH_3NH_3PbI_3$ Perovskite. *J. Phys. Chem. Lett.* **2015**, *6*, 1729−1735.
(48) Dang, Y.; Liu, Y.; Sun, Y.; Yuan, D.; Liu, X.; Lu, W.; Liu, G.; Xia, H.; Tao, X. Bulk Crystal Growth of Hybrid Perovskite Material $CH_3NH_3PbI_3$. *CrystEngComm* **2015**, *17*, 665−670.
(49) Weller, M. T.; Weber, O. J.; Henry, P. F.; Di Pumpo, A. M.; Hansen, T. C. Complete Structure and Cation Orientation in the Perovskite Photovoltaic Methylammonium Lead Iodide Between 100 and 352 K. *Chem. Commun.* **2015**, *51*, 4180−4183.
(50) Swainson, I.; Hammond, R.; Soullière, C.; Knop, O.; Massa, W. Phase Transitions in the Perovskite Methylammonium Lead Bromide, $CH_3ND_3PbBr_3$. *J. Solid State Chem.* **2003**, *176*, 97−104.
(51) Mosconi, E.; Quarti, C.; Ivanovska, T.; Ruani, G.; De Angelis, F. Structural and Electronic Properties of Organo-Halide Lead Perovskites: A Combined IR-Spectroscopy and Ab Initio Molecular Dynamics Investigation. *Phys. Chem. Chem. Phys.* **2014**, *16*, 16137−16144.
(52) Quarti, C.; Mosconi, E.; De Angelis, F. Structural and Electronic Properties of Organo-Halide Hybrid Perovskites from Ab Initio Molecular Dynamics. *Phys. Chem. Chem. Phys.* **2015**, *17*, 9394−9409.
(53) Carignano, M. A.; Kachmar, A.; Hutter, J. Thermal Effects on $CH_3NH_3PbI_3$ Perovskite from Ab Initio Molecular Dynamics Simulations. *J. Phys. Chem. C* **2015**, *119*, 8991−8997.
(54) Frost, J. M.; Butler, K. T.; Walsh, A. Molecular Ferroelectric Contributions to Anomalous Hysteresis in Hybrid Perovskite Solar Cells. *APL Mater.* **2014**, *2*, 081506.
(55) Leguy, A. M.; Frost, J. M.; McMahon, A. P.; Sakai, V. G.; Kochelmann, W.; Law, C.; Li, X.; Foglia, F.; Walsh, A.; Regan, B. C.; et al. The Dynamics of Methylammonium Ions in Hybrid Organic-Inorganic Perovskite Solar Cells. *Nat. Commun.* **2015**, *6*, 7124.
(56) Liu, S.; Zheng, F.; Koocher, N. Z.; Takenaka, H.; Wang, F.; Rappe, A. M. Ferroelectric Domain Wall Induced Band Gap Reduction and Charge Separation in Organometal Halide Perovskites. *J. Phys. Chem. Lett.* **2015**, *6*, 693−699.
(57) Ma, J.; Wang, L.-W. Nanoscale Charge Localization Induced by Random Orientations of Organic Molecules in Hybrid Perovskite $CH_3NH_3PbI_3$. *Nano Lett.* **2015**, *15*, 248−253.
(58) Poglitsch, A.; Weber, D. Dynamic Disorder in Methylammoniumtrihalogenoplumbates (II) Observed by Millimeter-Wave Spectroscopy. *J. Chem. Phys.* **1987**, *87*, 6373−6378.
(59) Wasylishen, R.; Knop, O.; Macdonald, J. Cation Rotation in Methylammonium Lead Halides. *Solid State Commun.* **1985**, *56*, 581−582.
(60) Even, J.; Pedesseau, L.; Jancu, J.-M.; Katan, C. Importance of Spin-Orbit Coupling in Hybrid Organic/Inorganic Perovskites for Photovoltaic Applications. *J. Phys. Chem. Lett.* **2013**, *4*, 2999−3005.
(61) Filip, M. R.; Giustino, F. *GW* Quasiparticle Band Gap of the Hybrid Organic−Inorganic Perovskite $CH_3NH_3PbI_3$: Effect of Spin-Orbit Interaction, Semicore Electrons, and Self-Consistency. *Phys. Rev. B: Condens. Matter Mater. Phys.* **2014**, *90*, 245145.
(62) Amat, A.; Mosconi, E.; Ronca, E.; Quarti, C.; Umari, P.; Nazeeruddin, M. K.; Graetzel, M.; De Angelis, F. Cation-Induced Band-Gap Tuning in Organohalide Perovskites: Interplay of Spin-Orbit Coupling and Octahedra Tilting. *Nano Lett.* **2014**, *14*, 3608−3616.
(63) Umari, P.; Mosconi, E.; De Angelis, F. Relativistic GW Calculations on $CH_3NH_3PbI_3$ and $CH_3NH_3SnI_3$ Perovskites for Solar Cell Applications. *Sci. Rep.* **2014**, *4*, 4467.
(64) Egger, D. A.; Kronik, L. Role of Dispersive Interactions in Determining Structural Properties of Organic−Inorganic Halide Perovskites: Insights from First-Principles Calculations. *J. Phys. Chem. Lett.* **2014**, *5*, 2728−2733.
(65) Kim, M.; Im, J.; Freeman, A. J.; Ihm, J.; Jin, H. Switchable $S = 1/2$ and $J = 1/2$ Rashba Bands in Ferroelectric Halide Perovskites. *Proc. Natl. Acad. Sci. U. S. A.* **2014**, *111*, 6900−6904.
(66) Motta, C.; El-Mellouhi, F.; Kais, S.; Tabet, N.; Alharbi, F.; Sanvito, S. Revealing the Role of Organic Cations in Hybrid Halide Perovskite $CH_3NH_3PbI_3$. *Nat. Commun.* **2015**, *6*, 7026.
(67) Zheng, F.; Tan, L. Z.; Liu, S.; Rappe, A. M. Rashba Spin-Orbit Coupling Enhanced Carrier Lifetime in Organometal Halide Perovskites. *Nano Lett.* **2015**, DOI: 10.1021/acs.nanolett.5b01854.
(68) Hsiao, Y.-C.; Wu, T.; Li, M.; Hu, B. Magneto-Optical Studies on Spin-Dependent Charge Recombination and Dissociation in Perovskite Solar Cells. *Adv. Mater.* **2015**, *27*, 2899−2906.
(69) Zhang, C.; Sun, D.; Sheng, C.-X.; Zhai, Y. X.; Mielczarek, K.; Vardeny, Z. V. Magnetic Field Effects in Hybrid Perovskite Devices. *Nat. Phys.* **2015**, *11*, 427−434.
(70) Takahashi, Y.; Obara, R.; Lin, Z.-Z.; Takahashi, Y.; Naito, T.; Inabe, T.; Ishibashi, S.; Terakura, K. Charge-Transport in Tin-Iodide Perovskite $CH_3NH_3SnI_3$: Origin of High Conductivity. *Dalton Trans.* **2011**, *40*, 5563−5568.
(71) Takahashi, Y.; Hasegawa, H.; Takahashi, Y.; Inabe, T. Hall Mobility in Tin Iodide Perovskite $CH_3NH_3SnI_3$: Evidence for a Doped Semiconductor. *J. Solid State Chem.* **2013**, *205*, 39−43.
(72) Pisoni, A.; Jaćimović, J.; Barišić, O. S.; Spina, M.; Gaál, R.; Forró, L.; Horváth, E. Ultra-Low Thermal Conductivity in Organic-Inorganic Hybrid Perovskite $CH_3NH_3PbI_3$. *J. Phys. Chem. Lett.* **2014**, *5*, 2488−2492.
(73) Shi, J.; Wei, H.; Lv, S.; Xu, X.; Wu, H.; Luo, Y.; Li, D.; Meng, Q. Control of Charge Transport in the Perovskite $CH_3NH_3PbI_3$ Thin Film. *ChemPhysChem* **2015**, *16*, 842−847.
(74) Deschler, F.; Price, M.; Pathak, S.; Klintberg, L. E.; Jarausch, D.-D.; Higler, R.; Huettner, S.; Leijtens, T.; Stranks, S. D.; Snaith, H. J.; et al. High Photoluminescence Efficiency and Optically Pumped Lasing in Solution-Processed Mixed Halide Perovskite Semiconductors. *J. Phys. Chem. Lett.* **2014**, *5*, 1421−1426.
(75) Tan, Z.-K.; Moghaddam, R. S.; Lai, M. L.; Docampo, P.; Higler, R.; Deschler, F.; Price, M.; Sadhanala, A.; Pazos, L. M.; Credgington, D.; et al. Bright Light-Emitting Diodes Based on Organometal Halide Perovskite. *Nat. Nanotechnol.* **2014**, *9*, 687−692.
(76) Xing, G.; Mathews, N.; Lim, S. S.; Yantara, N.; Liu, X.; Sabba, D.; Grätzel, M.; Mhaisalkar, S.; Sum, T. C. Low-Temperature Solution-Processed Wavelength-Tunable Perovskites for Lasing. *Nat. Mater.* **2014**, *13*, 476−480.
(77) Sutherland, B. R.; Hoogland, S.; Adachi, M. M.; Wong, C. T. O.; Sargent, E. H. Conformal Organohalide Perovskites Enable Lasing on Spherical Resonators. *ACS Nano* **2014**, *8*, 10947−10952.
(78) Zhang, Q.; Ha, S. T.; Liu, X.; Sum, T. C.; Xiong, Q. Room-Temperature Near-Infrared High-Q Perovskite Whispering-Gallery Planar Nanolasers. *Nano Lett.* **2014**, *14*, 5995−6001.
(79) Bass, K. K.; McAnally, R. E.; Zhou, S.; Djurovich, P. I.; Thompson, M. E.; Melot, B. C. Influence of Moisture on the Preparation, Crystal Structure, and Photophysical Properties of Organohalide Perovskites. *Chem. Commun.* **2014**, *50*, 15819−15822.
(80) Hailegnaw, B.; Kirmayer, S.; Edri, E.; Hodes, G.; Cahen, D. Rain on Methylammonium Lead Iodide Based Perovskites: Possible

DOI: 10.1021/acs.jpclett.5b01830
J. Phys. Chem. Lett. 2015, 6, 4862−4872

Environmental Effects of Perovskite Solar Cells. *J. Phys. Chem. Lett.* **2015**, *6*, 1543−1547.
(81) Niu, G.; Guo, X.; Wang, L. Review of Recent Progress in Chemical Stability of Perovskite Solar Cells. *J. Mater. Chem. A* **2015**, *3*, 8970−8980.
(82) Jung, H. S.; Park, N.-G. Perovskite Solar Cells: From Materials to Devices. *Small* **2015**, *11*, 10−25.
(83) Haruyama, J.; Sodeyama, K.; Han, L.; Tateyama, Y. Termination Dependence of Tetragonal $CH_3NH_3PbI_3$ Surfaces for Perovskite Solar Cells. *J. Phys. Chem. Lett.* **2014**, *5*, 2903−2909.
(84) Wang, Y.; Sumpter, B. G.; Huang, J.; Zhang, H.; Liu, P.; Yang, H.; Zhao, H. Density Functional Studies of Stoichiometric Surfaces of Orthorhombic Hybrid Perovskite $CH_3NH_3PbI_3$. *J. Phys. Chem. C* **2015**, *119*, 1136−1145.
(85) Niu, G.; Li, W.; Meng, F.; Wang, L.; Dong, H.; Qiu, Y. Study on the Stability of $CH_3NH_3PbI_3$ Films and the Effect of Post-Modification by Aluminum Oxide in All-Solid-State Hybrid Solar Cells. *J. Mater. Chem. A* **2014**, *2*, 705−710.
(86) Leguy, A. M. A.; Hu, Y.; Campoy-Quiles, M.; Alonso, M. I.; Weber, O. J.; Azarhoosh, P.; van Schilfgaarde, M.; Weller, M. T.; Bein, T.; Nelson, J.; et al. Reversible Hydration of $CH_3NH_3PbI_3$ in Films, Single Crystals, and Solar Cells. *Chem. Mater.* **2015**, *27*, 3397−3407.
(87) Christians, J. A.; Herrera, P. A. M.; Kamat, P. V. Transformation of the Excited State and Photovoltaic Efficiency of $CH_3NH_3PbI_3$ Perovskite upon Controlled Exposure to Humidified Air. *J. Am. Chem. Soc.* **2015**, *137*, 1530−1538.
(88) Yang, J.; Siempelkamp, B. D.; Liu, D.; Kelly, T. L. Investigation of $CH_3NH_3PbI_3$ Degradation Rates and Mechanisms in Controlled Humidity Environments Using *in Situ* Techniques. *ACS Nano* **2015**, *9*, 1955−1963.
(89) Mosconi, E.; Azpiroz, J. M.; De Angelis, F. Ab Initio Molecular Dynamics Simulations of Methylammonium Lead Iodide Perovskite Degradation by Water. *Chem. Mater.* **2015**, *27*, 4885−4892.
(90) Koocher, N. Z.; Edri, E.; Saldana-Greco, D.; Wang, F.; Liu, S.; Rappe, A. M. Polarization Dependence of Water Adsorption to $CH_3NH_3PbI_3$ (001) Surfaces. *J. Phys. Chem. Lett.* **2015**, *6*, 4371−4378.
(91) Smith, I. C.; Hoke, E. T.; Solis-Ibarra, D.; McGehee, M. D.; Karunadasa, H. I. A Layered Hybrid Perovskite Solar-Cell Absorber with Enhanced Moisture Stability. *Angew. Chem.* **2014**, *126*, 11414−11417.
(92) Jiang, Q.; Rebollar, D.; Gong, J.; Piacentino, E. L.; Zheng, C.; Xu, T. Pseudohalide-Induced Moisture Tolerance in Perovskite $CH_3NH_3Pb(SCN)_2I$ Thin Films. *Angew. Chem., Int. Ed.* **2015**, *54*, 7617−7620.
(93) Ito, S.; Tanaka, S.; Manabe, K.; Nishino, H. Effects of Surface Blocking Layer of Sb_2S_3 on Nanocrystalline TiO_2 for $CH_3NH_3PbI_3$ Perovskite Solar Cells. *J. Phys. Chem. C* **2014**, *118*, 16995−17000.
(94) Kempe, M. D.; Dameron, A. A.; Reese, M. O. Evaluation of Moisture Ingress from the Perimeter of Photovoltaic Modules. *Prog. Photovoltaics* **2014**, *22*, 1159−1171.
(95) Leijtens, T.; Eperon, G. E.; Pathak, S.; Abate, A.; Lee, M. M.; Snaith, H. J. Overcoming Ultraviolet Light Instability of Sensitized TiO_2 with Meso-Superstructured Organometal Tri-Halide Perovskite Solar Cells. *Nat. Commun.* **2013**, *4*, 2885.
(96) Li, W.; Dong, H.; Wang, L.; Li, N.; Guo, X.; Li, J.; Qiu, Y. Montmorillonite As Bifunctional Buffer Layer Material for Hybrid Perovskite Solar Cells with Protection from Corrosion and Retarding Recombination. *J. Mater. Chem. A* **2014**, *2*, 13587−13592.
(97) Tress, W.; Marinova, N.; Moehl, T.; Zakeeruddin, S.; Nazeeruddin, M. K.; Grätzel, M. Understanding the Rate-Dependent *J-V* Hysteresis, Slow Time Component, and Aging in $CH_3NH_3PbI_3$ Perovskite Solar Cells: The Role of a Compensated Electric Field. *Energy Environ. Sci.* **2015**, *8*, 995−1004.
(98) Kim, H.-S.; Park, N.-G. Parameters Affecting *I*−*V* Hysteresis of $CH_3NH_3PbI_3$ Perovskite Solar Cells: Effects of Perovskite Crystal Size and Mesoporous TiO_2 Layer. *J. Phys. Chem. Lett.* **2014**, *5*, 2927−2934.
(99) Chen, H.-W.; Sakai, N.; Ikegami, M.; Miyasaka, T. Emergence of Hysteresis and Transient Ferroelectric Response in Organo-Lead Halide Perovskite Solar Cells. *J. Phys. Chem. Lett.* **2015**, *6*, 164−169.
(100) Liu, C.; Fan, J.; Zhang, X.; Shen, Y.; Yang, L.; Mai, Y. Hysteretic Behavior upon Light Soaking in Perovskite Solar Cells Prepared Via Modified Vapor-Assisted Solution Process. *ACS Appl. Mater. Interfaces* **2015**, *7*, 9066−9071.
(101) Docampo, P.; Hanusch, F. C.; Giesbrecht, N.; Angloher, P.; Ivanova, A.; Bein, T. Influence of the Orientation of Methylammonium Lead Iodide Perovskite Crystals on Solar Cell Performance. *APL Mater.* **2014**, *2*, 081508−081513.
(102) Sanchez, R. S.; Gonzalez-Pedro, V.; Lee, J.-W.; Park, N.-G.; Kang, Y. S.; Mora-Sero, I.; Bisquert, J. Slow Dynamic Processes in Lead Halide Perovskite Solar Cells. Characteristic Times and Hysteresis. *J. Phys. Chem. Lett.* **2014**, *5*, 2357−2363.
(103) Egger, D. A.; Edri, E.; Cahen, D.; Hodes, G. Perovskite Solar Cells: Do We Know What We Do Not Know? *J. Phys. Chem. Lett.* **2015**, *6*, 279−282.
(104) Jena, A. K.; Chen, H.-W.; Kogo, A.; Sanehira, Y.; Ikegami, M.; Miyasaka, T. The Interface Between FTO and TiO_2 Compact Layer Can Be One of the Origins to Hysteresis in Planar Heterojunction Perovskite Solar Cells. *ACS Appl. Mater. Interfaces* **2015**, *7*, 9817−9823.
(105) Jeon, N. J.; Noh, J. H.; Kim, Y. C.; Yang, W. S.; Ryu, S.; Seok, S. I. Solvent Engineering for High-Performance Inorganic-Organic Hybrid Perovskite Solar Cells. *Nat. Mater.* **2014**, *13*, 897−903.
(106) Wu, X.; Trinh, M. T.; Niesner, D.; Zhu, H.; Norman, Z.; Owen, J. S.; Yaffe, O.; Kudisch, B. J.; Zhu, X. Trap States in Lead Iodide Perovskites. *J. Am. Chem. Soc.* **2015**, *137*, 2089−2096.
(107) Wojciechowski, K.; Stranks, S. D.; Abate, A.; Sadoughi, G.; Sadhanala, A.; Kopidakis, N.; Rumbles, G.; Li, C.-Z.; Friend, R. H.; Jen, A. K.-Y.; et al. Heterojunction Modification for Highly Efficient Organic-Inorganic Perovskite Solar Cells. *ACS Nano* **2014**, *8*, 12701−12709.
(108) Xu, J.; Buin, A.; Ip, A. H.; Li, W.; Voznyy, O.; Comin, R.; Yuan, M.; Jeon, S.; Ning, Z.; McDowell, J. J.; et al. Perovskite−Fullerene Hybrid Materials Suppress Hysteresis in Planar Diodes. *Nat. Commun.* **2015**, *6*, 7081.
(109) Shao, Y.; Xiao, Z.; Bi, C.; Yuan, Y.; Huang, J. Origin and Elimination of Photocurrent Hysteresis by Fullerene Passivation in $CH_3NH_3PbI_3$ Planar Heterojunction Solar Cells. *Nat. Commun.* **2014**, *5*, 5784.
(110) Abate, A.; Saliba, M.; Hollman, D. J.; Stranks, S. D.; Wojciechowski, K.; Avolio, R.; Grancini, G.; Petrozza, A.; Snaith, H. J. Supramolecular Halogen Bond Passivation of Organic-Inorganic Halide Perovskite Solar Cells. *Nano Lett.* **2014**, *14*, 3247−3254.
(111) Nagaoka, H.; Ma, F.; deQuilettes, D. W.; Vorpahl, S. M.; Glaz, M. S.; Colbert, A. E.; Ziffer, M. E.; Ginger, D. S. Zr Incorporation into TiO_2 Electrodes Reduces Hysteresis and Improves Performance in Hybrid Perovskite Solar Cells While Increasing Carrier Lifetimes. *J. Phys. Chem. Lett.* **2015**, *6*, 669−675.
(112) Nie, W.; Tsai, H.; Asadpour, R.; Blancon, J.-C.; Neukirch, A. J.; Gupta, G.; Crochet, J. J.; Chhowalla, M.; Tretiak, S.; Alam, M. A.; et al. High-Efficiency Solution-Processed Perovskite Solar Cells with Millimeter-Scale Grains. *Science* **2015**, *347*, 522−525.
(113) Young, S. M.; Rappe, A. M. First Principles Calculation of the Shift Current Photovoltaic Effect in Ferroelectrics. *Phys. Rev. Lett.* **2012**, *109*, 116601−116605.
(114) Young, S. M.; Zheng, F.; Rappe, A. M. First-Principles Calculation of the Bulk Photovoltaic Effect in Bismuth Ferrite. *Phys. Rev. Lett.* **2012**, *109*, 236601−236605.
(115) Hoke, E. T.; Slotcavage, D. J.; Dohner, E. R.; Bowring, A. R.; Karunadasa, H. I.; McGehee, M. D. Reversible Photo-Induced Trap Formation in Mixed-Halide Hybrid Perovskites for Photovoltaics. *Chem. Sci.* **2015**, *6*, 613−617.
(116) Wu, X.; Yu, H.; Li, L.; Wang, F.; Xu, H.; Zhao, N. Composition-Dependent Light-Induced Dipole Moment Change in Organometal Halide Perovskites. *J. Phys. Chem. C* **2015**, *119*, 1253−1259.
(117) Gottesman, R.; Haltzi, E.; Gouda, L.; Tirosh, S.; Bouhadana, Y.; Zaban, A.; Mosconi, E.; De Angelis, F. Extremely Slow Photoconductivity Response of $CH_3NH_3PbI_3$ Perovskites Suggesting

DOI: 10.1021/acs.jpclett.5b01830
J. Phys. Chem. Lett. 2015, 6, 4862−4872

Structural Changes Under Working Conditions. *J. Phys. Chem. Lett.* **2014**, *5*, 2662−2669.
(118) Goldschmidt, V. M. Die Gesetzte Der Krystallochemie. *Naturwissenschaften* **1926**, *14*, 477−485.
(119) Muller, O. *The Major Ternary Structural Families (Crystal Chemistry of Non-Metallic Materials)*; Springer: New York, 1974.
(120) Pettifor, D. A. Chemical Scale for Crystal-Structure Maps. *Solid State Commun.* **1984**, *51*, 31−34.
(121) Brehm, J. A.; Bennett, J. W.; Schoenberg, M. R.; Grinberg, I.; Rappe, A. M. The Structural Diversity of ABS_3 Compounds with d0 Electronic Configuration for the B-cation. *J. Chem. Phys.* **2014**, *140*, 224703.
(122) Kieslich, G.; Sun, S.; Cheetham, A. K. Solid-State Principles Applied to Organic-Inorganic Perovskites: New Tricks for an Old Dog. *Chem. Sci.* **2014**, *5*, 4712−4715.
(123) Kieslich, G.; Sun, S.; Cheetham, A. K. An Extended Tolerance Factor Approach for Organic-Inorganic Perovskites. *Chem. Sci.* **2015**, *6*, 3430−3433.
(124) Lee, J.-W.; Seol, D.-J.; Cho, A.-N.; Park, N.-G. High-Efficiency Perovskite Solar Cells Based on the Black Polymorph of $HC(NH_2)_2PbI_3$. *Adv. Mater.* **2014**, *26*, 4991−4998.
(125) Koh, T. M.; Fu, K.; Fang, Y.; Chen, S.; Sum, T. C.; Mathews, N.; Mhaisalkar, S. G.; Boix, P. P.; Baikie, T. Formamidinium-Containing Metal-Halide: An Alternative Material for Near-IR Absorption Perovskite Solar Cells. *J. Phys. Chem. C* **2014**, *118*, 16458−16462.
(126) Pellet, N.; Gao, P.; Gregori, G.; Yang, T.-Y.; Nazeeruddin, M. K.; Maier, J.; Grätzel, M. Mixed-Organic-Cation Perovskite Photovoltaics for Enhanced Solar-Light Harvesting. *Angew. Chem., Int. Ed.* **2014**, *53*, 3151−3157.
(127) Giorgi, G.; Fujisawa, J.-I.; Segawa, H.; Yamashita, K. Organic-Inorganic Hybrid Lead Iodide Perovskite Featuring Zero Dipole Moment Guanidinium Cations: A Theoretical Analysis. *J. Phys. Chem. C* **2015**, *119*, 4694−4701.
(128) Chung, I.; Song, J.-H.; Im, J.; Androulakis, J.; Malliakas, C. D.; Li, H.; Freeman, A. J.; Kenney, J. T.; Kanatzidis, M. G. $CsSnI_3$: Semiconductor or Metal? High Electrical Conductivity and Strong Near-Infrared Photoluminescence from a Single Material. High Hole Mobility and Phase-Transitions. *J. Am. Chem. Soc.* **2012**, *134*, 8579−8587.
(129) Chung, I.; Lee, B.; He, J.; Chang, R. P. H.; Kanatzidis, M. G. All-Solid-State Dye-Sensitized Solar Cells with High Efficiency. *Nature* **2012**, *485*, 486−489.
(130) Hao, F.; Stoumpos, C. C.; Chang, R. P. H.; Kanatzidis, M. G. Anomalous Band Gap Behavior in Mixed Sn and Pb Perovskites Enables Broadening of Absorption Spectrum in Solar Cells. *J. Am. Chem. Soc.* **2014**, *136*, 8094−8099.
(131) Stoumpos, C. C.; Frazer, L.; Clark, D. J.; Kim, Y. S.; Rhim, S. H.; Freeman, A. J.; Ketterson, J. B.; Jang, J. I.; Kanatzidis, M. G. Hybrid Germanium Iodide Perovskite Semiconductors: Active Lone Pairs, Structural Distortions, Direct and Indirect Energy Gaps, and Strong Nonlinear Optical Properties. *J. Am. Chem. Soc.* **2015**, *137*, 6804−6819.
(132) Hao, F.; Stoumpos, C. C.; Cao, D. H.; Chang, R. P. H.; Kanatzidis, M. G. Lead-Free Solid-State Organic-Inorganic Halide Perovskite Solar Cells. *Nat. Photonics* **2014**, *8*, 489−494.
(133) Noel, N. K.; Stranks, S. D.; Abate, A.; Wehrenfennig, C.; Guarnera, S.; Haghighirad, A.-A.; Sadhanala, A.; Eperon, G. E.; Pathak, S. K.; Johnston, M. B.; et al. Lead-Free Organic-Inorganic Tin Halide Perovskites for Photovoltaic Applications. *Energy Environ. Sci.* **2014**, *7*, 3061−3068.
(134) Ogomi, Y.; Morita, A.; Tsukamoto, S.; Saitho, T.; Fujikawa, N.; Shen, Q.; Toyoda, T.; Yoshino, K.; Pandey, S. S.; Ma, T.; et al. $CH_3NH_3Sn_xPb_{(1-X)}I_3$ Perovskite Solar Cells Covering up to 1060 nm. *J. Phys. Chem. Lett.* **2014**, *5*, 1004−1011.
(135) Mosconi, E.; Umari, P.; De Angelis, F. Electronic and Optical Properties of Mixed Sn-Pb Organohalide Perovskites: A First Principles Investigation. *J. Mater. Chem. A* **2015**, *3*, 9208−9215.
(136) Zuo, F.; Williams, S. T.; Liang, P.-W.; Chueh, C.-C.; Liao, C.-Y.; Jen, A. K.-Y. Binary-Metal Perovskites Toward High-Performance Planar-Heterojunction Hybrid Solar Cells. *Adv. Mater.* **2014**, *26*, 6454−6460.
(137) Dharani, S.; Dewi, H. A.; Prabhakar, R. R.; Baikie, T.; Shi, C.; Yonghua, D.; Mathews, N.; Boix, P. P.; Mhaisalkar, S. G. Incorporation of Cl into Sequentially Deposited Lead Halide Perovskite Films for Highly Efficient Mesoporous Solar Cells. *Nanoscale* **2014**, *6*, 13854−13860.
(138) Tidhar, Y.; Edri, E.; Weissman, H.; Zohar, D.; Hodes, G.; Cahen, D.; Rybtchinski, B.; Kirmayer, S. Crystallization of Methyl Ammonium Lead Halide Perovskites: Implications for Photovoltaic Applications. *J. Am. Chem. Soc.* **2014**, *136*, 13249−13256.
(139) Mostafa, M.; Semary, M.; Ahmed, M. Field Dependence of the Susceptibility Maximum for Two-Dimensional Antiferromagnet. *Phys. Lett. A* **1977**, *61*, 183−184.
(140) Mostafa, M. F.; Willett, R. D. Magnetic Properties of Ferrous Chloride Complexes with Two-Dimensional Structures. *Phys. Rev. B* **1971**, *4*, 2213−2215.
(141) Semary, M.; Mostafa, M.; Ahmed, M. Magnetic Susceptibility of $(CH_3NH_3)_2FeCl_3Br$: An Example of a Canted Spin System. *Solid State Commun.* **1978**, *25*, 443−445.
(142) Han, J.; Nishihara, S.; Inoue, K.; Kurmoo, M. On the Nature of the Structural and Magnetic Phase Transitions in the Layered Perovskite-like $(CH_3NH_3)_2[FeIICl_4]$. *Inorg. Chem.* **2014**, *53*, 2068−2075.
(143) Arend, H.; Huber, W.; Mischgofsky, F.; Richter-Van Leeuwen, G. R. Layer Perovskites of the $(C_nH_{2n+1}NH_3)_2MX_4$ and $NH_3(CH_2)_mNH_3MX_4$ Families with M = Cd, Cu, Fe, Mn or Pd and X = Cl or Br: Importance, Solubilities and Simple Growth Techniques. *J. Cryst. Growth* **1978**, *43*, 213−223.
(144) Cheng, Z.; Lin, J. Layered Organic-Inorganic Hybrid Perovskites: Structure, Optical Properties, Film Preparation, Patterning and Templating Engineering. *CrystEngComm* **2010**, *12*, 2646−2662.
(145) Dohner, E. R.; Hoke, E. T.; Karunadasa, H. I. Self-Assembly of Broadband White-Light Emitters. *J. Am. Chem. Soc.* **2014**, *136*, 1718−1721.
(146) Dohner, E. R.; Jaffe, A.; Bradshaw, L. R.; Karunadasa, H. I. Intrinsic White-Light Emission from Layered Hybrid Perovskites. *J. Am. Chem. Soc.* **2014**, *136*, 13154−13157.
(147) Lee, B.; Stoumpos, C. C.; Zhou, N.; Hao, F.; Malliakas, C.; Yeh, C.-Y.; Marks, T. J.; Kanatzidis, M. G.; Chang, R. P. H. Air-Stable Molecular Semiconducting Iodosalts for Solar Cell Applications: Cs_2SnI_6 as a Hole Conductor. *J. Am. Chem. Soc.* **2014**, *136*, 15379−15385.
(148) Schmidt, L. C.; Pertegás, A.; González-Carrero, S.; Malinkiewicz, O.; Agouram, S.; Mínguez Espallargas, G.; Bolink, H. J.; Galian, R. E.; Pérez-Prieto, J. Nontemplate Synthesis of $CH_3NH_3PbBr_3$ Perovskite Nanoparticles. *J. Am. Chem. Soc.* **2014**, *136*, 850−853.
(149) Tyagi, P.; Arveson, S. M.; Tisdale, W. A. Colloidal Organohalide Perovskite Nanoplatelets Exhibiting Quantum Confinement. *J. Phys. Chem. Lett.* **2015**, *6*, 1911−1916.
(150) Muthu, C.; Nagamma, S. R.; Nair, V. C. Luminescent Hybrid Perovskite Nanoparticles As a New Platform for Selective Detection of 2,4,6-Trinitrophenol. *RSC Adv.* **2014**, *4*, 55908−55911.
(151) Chen, Z.; Li, H.; Tang, Y.; Huang, X.; Ho, D.; Lee, C.-S. Shape-Controlled Synthesis of Organolead Halide Perovskite Nanocrystals and Their Tunable Optical Absorption. *Mater. Res. Express* **2014**, *1*, 015034−015043.

DOI: 10.1021/acs.jpclett.5b01830
J. Phys. Chem. Lett. 2015, 6, 4862−4872